# 6 Appendix

The Appendix contains the meandering patterns and ionic conductances of the simulations. Furthermore, the PM and DGM parameters are given and the optimisation strategy is demonstrated for DGM. Finally, additional results regarding the performance metrics precision, recall, and $F_2$-score are visually illustrated, discussed, and listed in tables.

## 6.1 Meandering patterns of the rotor tips

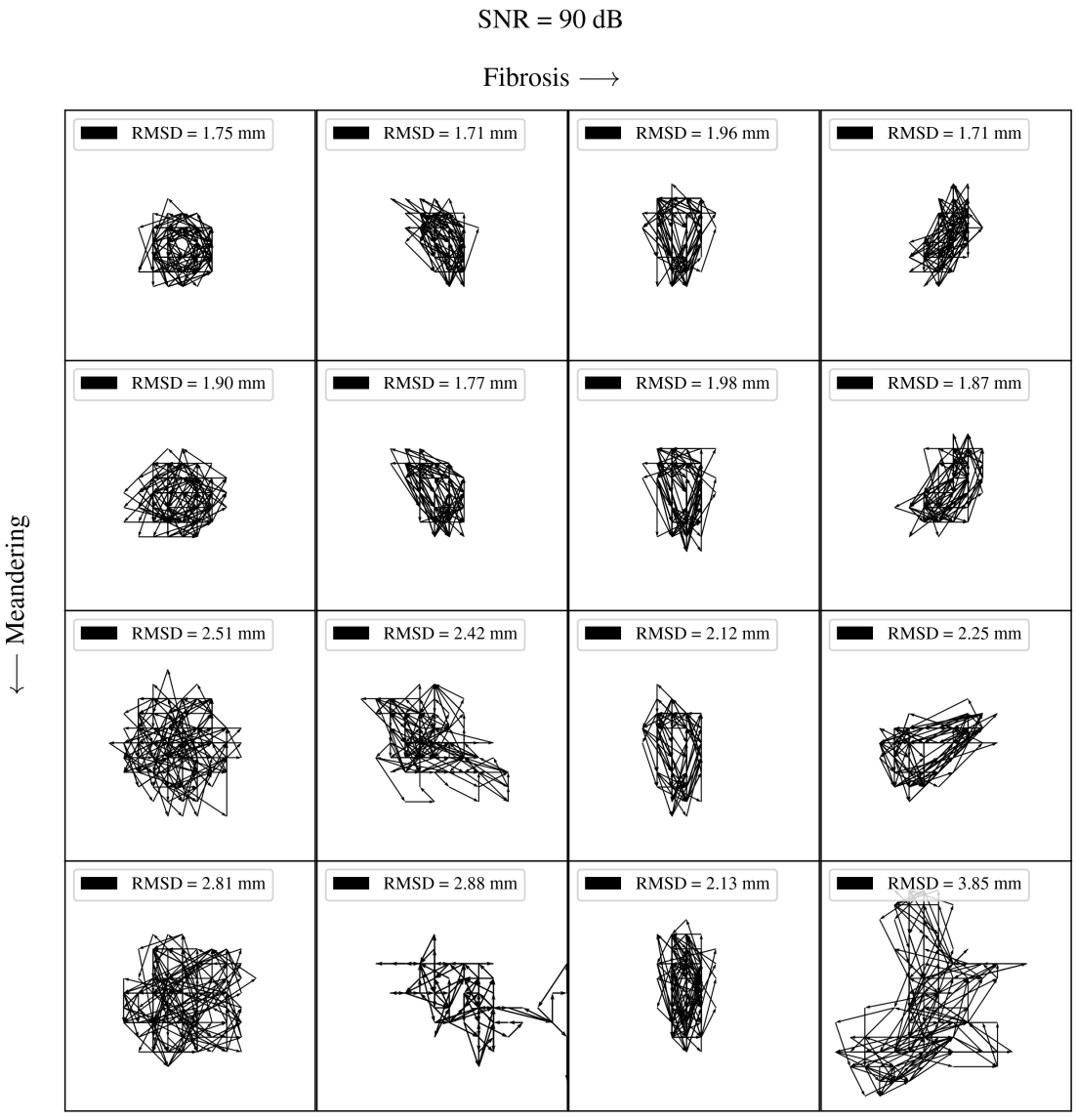


Figure 11: Illustration of the meandering patterns of rotor tip and RMSD values in mm (section 2.1).

## 6.2 Conductances of different meandering rotors

Table 4: Table illustrating the varied ionic conductances for various levels of meandering (section 2.1).

| rotor (row, column) | fibrosis [%] | $G_{\mathrm{Ca}}$ [mS/cm$^2$] | $G_{\mathrm{Na}}$ [mS/cm$^2$] | $G_{\mathrm{K}}$ [mS/cm$^2$] | RMSD [mm] |
|---|---|---|---|---|---|
| (1, 1) | 0 | 0 | 22 | 0.423 | 1.75 |
| (2, 1) | 0 | 0 | 14 | 0.423 | 1.90 |
| (3, 1) | 0 | 0.02 | 14 | 0.423 | 2.51 |
| (4, 1) | 0 | 0.02 | 22 | 0.423 | 2.81 |
| (1, 2) | 10 | 0 | 22 | 0.423 | 1.71 |
| (2, 2) | 10 | 0 | 14 | 0.423 | 1.77 |
| (3, 2) | 10 | 0.02 | 22 | 0.423 | 2.42 |
| (4, 2) | 10 | 0.02 | 14 | 0.423 | 2.88 |
| (1, 3) | 20 | 0 | 14 | 0.423 | 1.96 |
| (2, 3) | 20 | 0 | 22 | 0.423 | 1.98 |
| (3, 3) | 20 | 0.02 | 14 | 0.423 | 2.12 |
| (4, 3) | 20 | 0.02 | 22 | 0.423 | 2.13 |
| (1, 4) | 30 | 0 | 22 | 0.423 | 1.71 |
| (2, 4) | 30 | 0.02 | 14 | 0.423 | 1.87 |
| (3, 4) | 30 | 0 | 14 | 0.423 | 2.25 |
| (4, 4) | 30 | 0.02 | 22 | 0.423 | 3.85 |

## 6.3 PM and DGM parameters

The following tables depict PM and DGM parameters for the 2D simulations. The PM parameters were fine-tuned by trial and error without cross-validation. The parameters concerning rotor detection and clustering were initially selected to be the optimal parameters found in Li et al. [39]. These parameters were varied slightly to obtain the optimal results for the 2D simulations.

Table 5: Table listing the optimal PM parameters (section 2.2).

| | |
|---|---|
| ST window | 40 ms |
| HT band pass | [40 Hz, 250 Hz] (order 3) |
| HT low pass | 30 Hz (order 8) |
| HT window scale | 0.90 |
| 2D convolution kernel | 3x3 nabla |
| topological charge threshold | $\pm$ 0.95 |
| phase threshold | $\pm$ 1.5$\pi$ |
| DBSCAN min_samples | 3 |
| DBSCAN $\varepsilon$ | $\sqrt{2}d_{\text{mesh}} = 1.237$ mm |

Table 6: Table listing the optimal DGM parameters (section 2.3).

| | |
|---|---|
| $\Delta r_{\max}$ | 2.0 mm |
| $\Delta\text{LAT}_{\max}$ | 100 ms |
| $\text{CV}_{\min}$ | 0.2 $\frac{\text{mm}}{\text{ms}}$ |
| $\text{CV}_{\max}$ | 2.0 $\frac{\text{mm}}{\text{ms}}$ |
| $\Delta t_{\text{merge}}$ | 10 ms |
| DBSCAN min_samples | 25 |
| DBSCAN $\varepsilon$ | $\sqrt{2}d_{\text{mesh}} = 1.237$ mm |

Current parameter selection for DGM relies primarily on physiological considerations, acknowledging the speculative nature of this approach. To address this limitation, alternative methods for constructing graphs that are less reliant on specific parameter choices are actively explored. Additionally, the authors of this paper are working on developing parameter optimisation tools. As part of efforts to enhance the robustness of the DGM methodology, further parameter optimisation for this paper was conducted. This involved systematically adjusting parameters by iteratively doubling or halving their values to investigate the parameter sensitivity of DGM. The resulting $F_2$-scores were maximised through this iterative exploration, leading to the identification of an optimal parameter set. Seven values for each of the six parameters ($\Delta r_{\max}$, $\Delta\text{LAT}_{\max}$, $\Delta t_{\text{merge}}$, $\text{CV}_{\min}$, $\text{CV}_{\max}$, and DBSCAN min_samples) were considered, resulting in a total of 37 combinations.

While a comprehensive search across the entire parameter space for all 64 simulations is beyond the scope of this paper, its potential value for future research is acknowledged. Nevertheless, an analysis of parameter influence on the $F_2$-scores for one challenging simulation is presented, focusing on the most difficult rotor characterised by high meandering, fibrosis, and noise. Figure 12 illustrates the relationship between $F_2$-score and DGM parameter values for this challenging rotor. The interpretation of parameter effects on $F_2$-scores reveals notable findings.

The distance parameter exhibits a strong influence, with values that are too low resulting in insufficient graph connections, and values that are too high leading to an excessive number of long-range connections, both contributing to a decline in performance. The $\Delta\text{LAT}_{\text{max}}$ parameter, on the other hand, has minimal impact on scores, as its values are never exceeded due to the similarity of neighbouring points in terms of LAT values. The $\Delta t_{\text{merge}}$ parameter demonstrates a peak around 10, a value associated with the cycle length. Rotors with a minimum cycle length of 40 ms suggest that scores may decrease when approaching $\Delta t_{\text{merge}} = 20$ ms, as the graph merge interval length of $2\Delta t_{\text{merge}}$ exceeds the minimum cycle length. Values below 10 ms result in fewer connected graphs, leading to fewer detected cycles. $\text{CV}_{\text{min}}$ and $\text{CV}_{\text{max}}$ exhibit a strong dependence, influencing the number of connections filtered in or out of the graph. Optimal intervals for these parameters are expected to be closely tied to the physiological aspects of the problem, as neglecting regions of slow or fast conduction directly impacts performance. Lastly, the DBSCAN min_samples parameter displays a pronounced dependence, with greater values leading to more neglected detections. In this case, cluster sizes tend to be smaller than the DBSCAN min_samples value, resulting in fewer detections and lower $F_2$-scores. In summary, the exploration of parameter sensitivity and its impact on $F_2$-scores provides valuable insights into the relationships between parameter choices and the performance of DGM, contributing to a more informed and optimised approach.

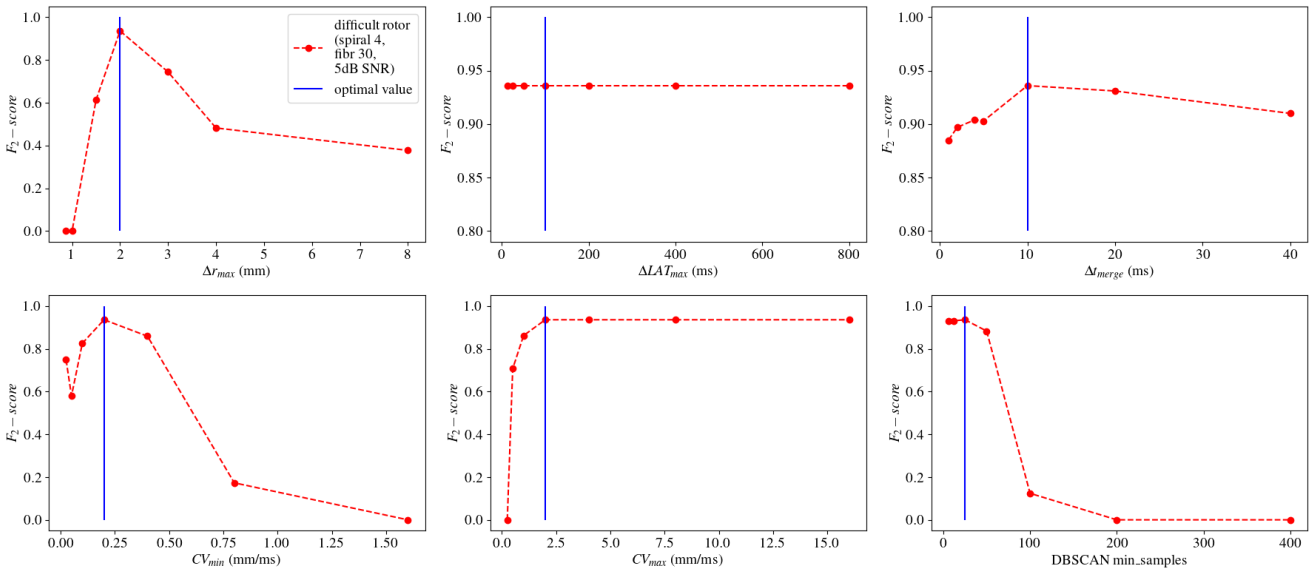


Figure 12: $F_2$-score vs DGM parameter values for a difficult rotor.

## 6.4 Precision

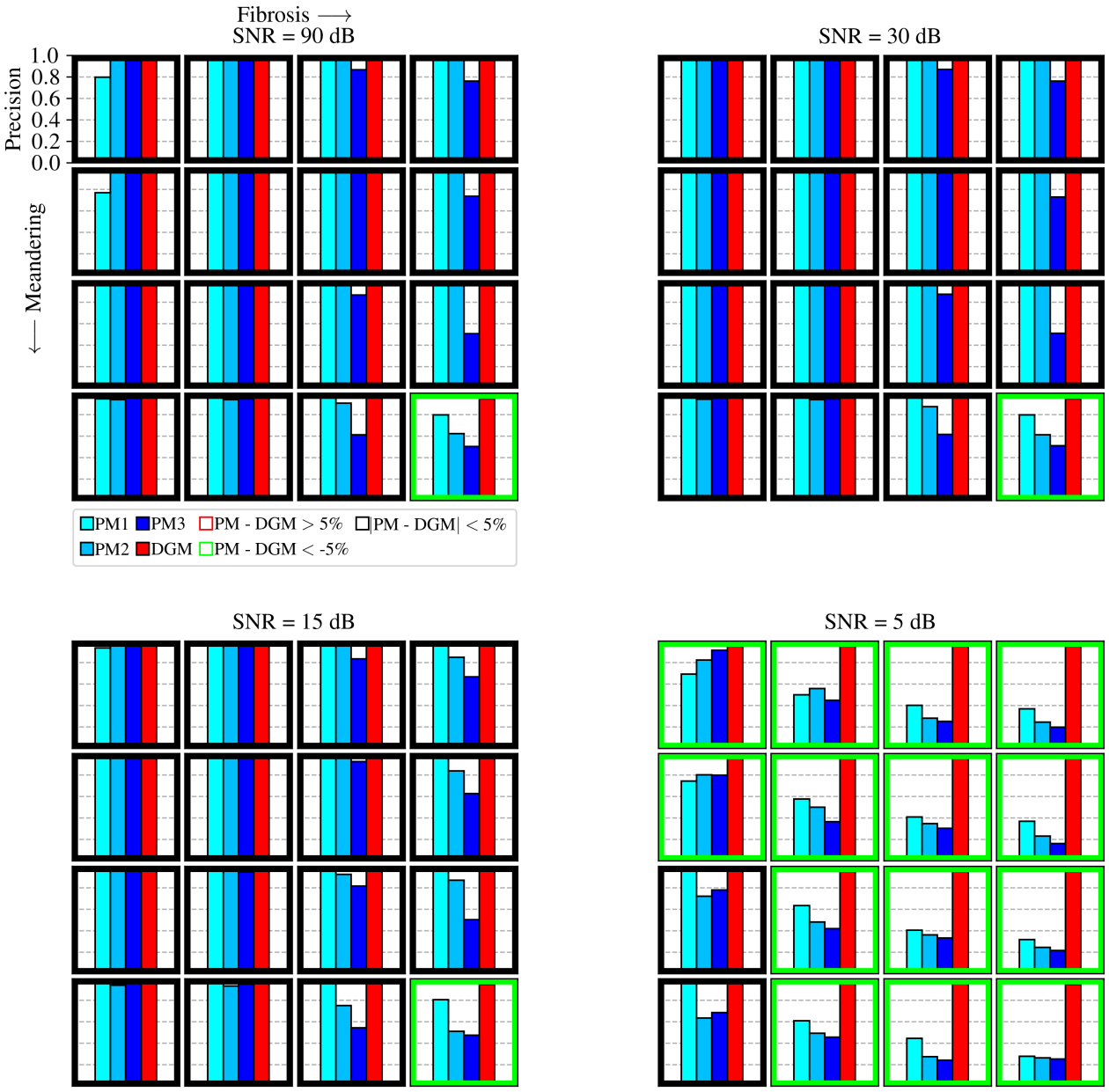


Figure 13: Illustration of the precision values for the full duration of all 64 simulations for the four rotor detection methods. The coloured squares around each plot show if the best PM method is better than, equal to or worse than DGM (red, **black**, green respectively) where a threshold of 5% is chosen.

The precision values depend exclusively on the amount of TP and FP. Low values are indicative of an excess of detections that are not related to the true rotor. Large performance drops are observed for all PM methods as fibrosis, meandering and noise are increased as seen in Figure 13. This is again indicative of the large amount of FP generated by PM in these conditions. The PM method with the highest precision (PM1), drops as low as

0.275 for the highest meandering, fibrosis and noise rotor. This is in sheer contrast with DGM, which retains a precision above 0.948 for all simulations.

Table 7: Precision of different PM methods and DGM for all 64 2D rotor simulations with various amounts of meandering, fibrosis and noise. Minimal values are marked in blue (PM) and red (DGM).

| rotor (row, column) | Pr(PM1) | Pr(PM2) | Pr(PM3) | Pr(DGM) | rotor (row, column) | Pr(PM1) | Pr(PM2) | Pr(PM3) | Pr(DGM) |
|---|---|---|---|---|---|---|---|---|---|
| (1, 1) | 0.796 | 1.000 | 1.000 | 1.000 | (1, 5) | 0.990 | 1.000 | 1.000 | 1.000 |
| (1, 2) | 1.000 | 1.000 | 1.000 | 1.000 | (1, 6) | 1.000 | 1.000 | 1.000 | 1.000 |
| (1, 3) | 1.000 | 1.000 | 0.867 | 1.000 | (1, 7) | 1.000 | 1.000 | 0.870 | 1.000 |
| (1, 4) | 1.000 | 1.000 | 0.761 | 1.000 | (1, 8) | 1.000 | 1.000 | 0.758 | 1.000 |
| (2, 1) | 0.767 | 1.000 | 0.989 | 1.000 | (2, 5) | 1.000 | 1.000 | 1.000 | 1.000 |
| (2, 2) | 1.000 | 1.000 | 1.000 | 1.000 | (2, 6) | 1.000 | 1.000 | 1.000 | 1.000 |
| (2, 3) | 1.000 | 1.000 | 1.000 | 1.000 | (2, 7) | 1.000 | 1.000 | 1.000 | 1.000 |
| (2, 4) | 1.000 | 0.985 | 0.737 | 1.000 | (2, 8) | 1.000 | 0.990 | 0.730 | 1.000 |
| (3, 1) | 1.000 | 0.961 | 1.000 | 0.979 | (3, 5) | 1.000 | 0.956 | 1.000 | 0.979 |
| (3, 2) | 0.990 | 0.979 | 0.962 | 1.000 | (3, 6) | 1.000 | 0.974 | 0.957 | 1.000 |
| (3, 3) | 1.000 | 0.995 | 0.866 | 0.995 | (3, 7) | 1.000 | 1.000 | 0.873 | 0.995 |
| (3, 4) | 0.995 | 1.000 | 0.503 | 1.000 | (3, 8) | 0.995 | 1.000 | 0.508 | 1.000 |
| (4, 1) | 0.946 | 0.938 | 0.995 | 0.969 | (4, 5) | 0.985 | 0.942 | 1.000 | 0.964 |
| (4, 2) | 1.000 | 0.939 | 0.948 | 1.000 | (4, 6) | 1.000 | 0.939 | 0.948 | 1.000 |
| (4, 3) | 0.995 | 0.905 | 0.611 | 1.000 | (4, 7) | 0.995 | 0.872 | 0.617 | 1.000 |
| (4, 4) | 0.798 | 0.621 | 0.504 | 0.948 | (4, 8) | 0.796 | 0.613 | 0.510 | 0.948 |
| (5, 1) | 0.933 | 0.970 | 0.989 | 1.000 | (5, 5) | 0.691 | 0.823 | 0.914 | 1.000 |
| (5, 2) | 1.000 | 1.000 | 1.000 | 1.000 | (5, 6) | 0.496 | 0.556 | 0.447 | 1.000 |
| (5, 3) | 1.000 | 0.970 | 0.834 | 1.000 | (5, 7) | 0.398 | 0.278 | 0.249 | 1.000 |
| (5, 4) | 1.000 | 0.848 | 0.664 | 1.000 | (5, 8) | 0.367 | 0.243 | 0.195 | 1.000 |
| (6, 1) | 1.000 | 0.990 | 0.984 | 1.000 | (6, 5) | 0.743 | 0.802 | 0.798 | 1.000 |
| (6, 2) | 1.000 | 1.000 | 0.977 | 1.000 | (6, 6) | 0.574 | 0.501 | 0.364 | 1.000 |
| (6, 3) | 1.000 | 0.985 | 0.926 | 1.000 | (6, 7) | 0.409 | 0.347 | 0.301 | 1.000 |
| (6, 4) | 1.000 | 0.839 | 0.625 | 1.000 | (6, 8) | 0.367 | 0.231 | 0.159 | 1.000 |
| (7, 1) | 1.000 | 0.951 | 0.994 | 0.985 | (7, 5) | 0.995 | 0.720 | 0.779 | 0.985 |
| (7, 2) | 0.995 | 0.960 | 0.945 | 1.000 | (7, 6) | 0.632 | 0.479 | 0.416 | 1.000 |
| (7, 3) | 0.985 | 0.924 | 0.814 | 0.990 | (7, 7) | 0.404 | 0.358 | 0.328 | 0.985 |
| (7, 4) | 0.990 | 0.867 | 0.502 | 1.000 | (7, 8) | 0.314 | 0.244 | 0.213 | 0.990 |
| (8, 1) | 0.985 | 0.938 | 0.984 | 0.959 | (8, 5) | 0.990 | 0.635 | 0.683 | 0.959 |
| (8, 2) | 1.000 | 0.932 | 0.950 | 1.000 | (8, 6) | 0.608 | 0.490 | 0.455 | 1.000 |
| (8, 3) | 0.995 | 0.750 | 0.542 | 1.000 | (8, 7) | 0.443 | 0.272 | 0.239 | 0.995 |
| (8, 4) | 0.803 | 0.511 | 0.473 | 0.948 | (8, 8) | 0.275 | 0.261 | 0.251 | 0.948 |

## 6.5 Recall

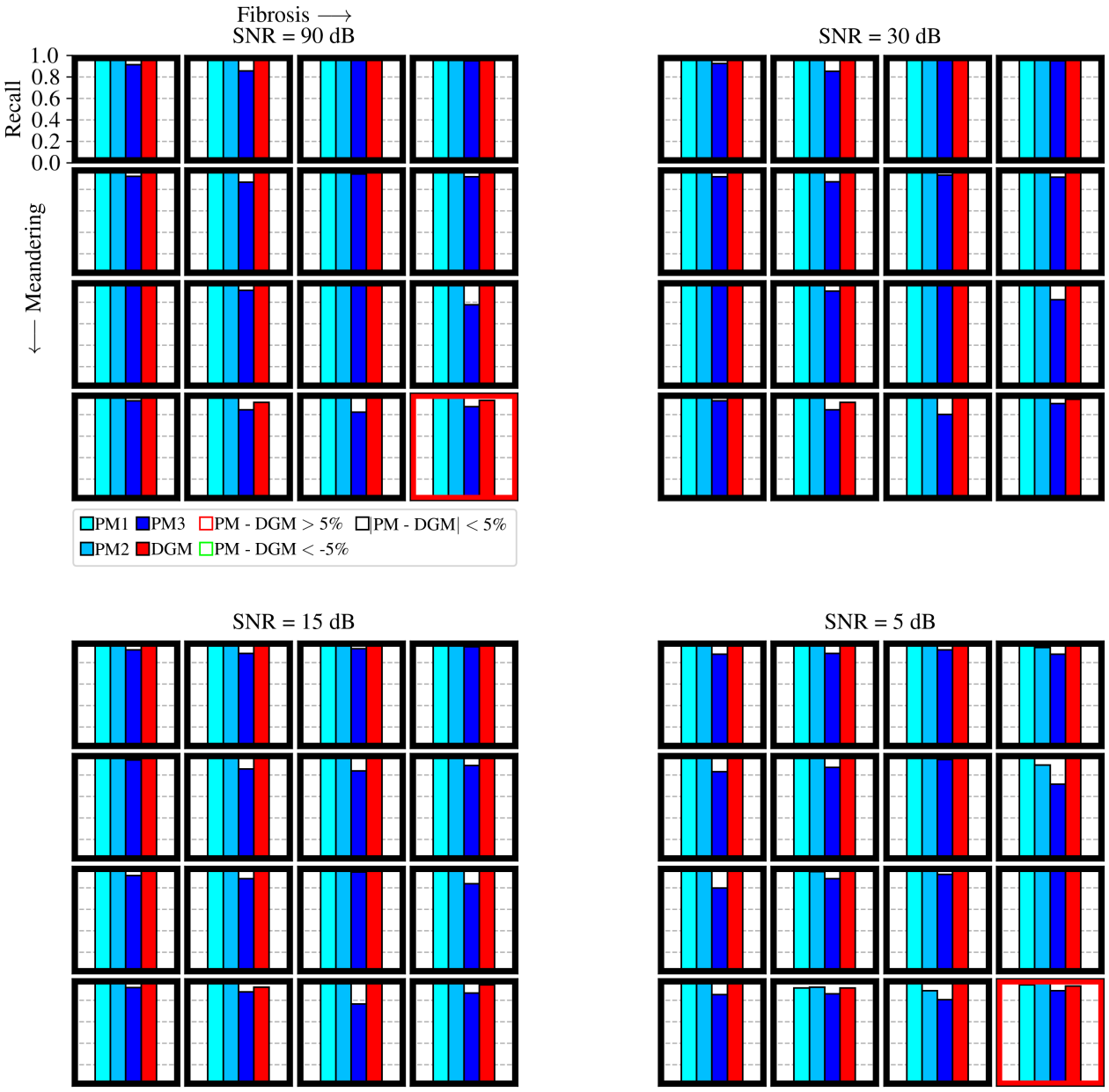


Figure 14: Illustration of the recall values for the full duration of all 64 simulations for the four rotor detection methods. The coloured squares around each plot show if the best PM method is better than, equal to or worse than DGM (red, **black**, green respectively) where a threshold of 5% is chosen.

The recall values depend only on the amount of TP and FN. Low values indicate an excessive amount of cases where the true rotor goes unnoticed. This value appears to be very high for all methods. However, recall values of PM3 drop more for increasing fibrosis, meandering and noise as compared to PM1, PM2 and DGM. The best PM method and DGM achieve recall values above 0.915. High recall values are expected for the PM methods as

they generate many FPs, which decreases the chance of cases containing a high number of FN. In this sense, the performance difference between PM and DGM cannot be explained from the recall value alone. Figure 13 and 14 clearly illustrate that precision is the main contributor to the performance difference between PM and DGM.

Table 8: Table listing recall of different PM methods and DGM for all 64 2D rotor simulations with various amounts of meandering, fibrosis and noise. Minimal values are marked in blue (PM) and red (DGM).

| rotor (row, column) | Re(PM1) | Re(PM2) | Re(PM3) | Re(DGM) | rotor (row, column) | Re(PM1) | Re(PM2) | Re(PM3) | Re(DGM) |
|---|---|---|---|---|---|---|---|---|---|
| (1, 1) | 1.000 | 1.000 | 0.913 | 1.000 | (1, 5) | 1.000 | 1.000 | 0.923 | 1.000 |
| (1, 2) | 1.000 | 1.000 | 0.856 | 1.000 | (1, 6) | 1.000 | 1.000 | 0.851 | 1.000 |
| (1, 3) | 1.000 | 1.000 | 0.969 | 1.000 | (1, 7) | 1.000 | 1.000 | 0.964 | 1.000 |
| (1, 4) | 1.000 | 1.000 | 0.949 | 1.000 | (1, 8) | 1.000 | 1.000 | 0.949 | 1.000 |
| (2, 1) | 0.995 | 1.000 | 0.923 | 1.000 | (2, 5) | 1.000 | 1.000 | 0.918 | 1.000 |
| (2, 2) | 1.000 | 1.000 | 0.867 | 1.000 | (2, 6) | 1.000 | 1.000 | 0.872 | 1.000 |
| (2, 3) | 1.000 | 1.000 | 0.944 | 1.000 | (2, 7) | 1.000 | 1.000 | 0.933 | 1.000 |
| (2, 4) | 1.000 | 0.985 | 0.918 | 1.000 | (2, 8) | 1.000 | 0.990 | 0.913 | 1.000 |
| (3, 1) | 1.000 | 1.000 | 0.954 | 0.979 | (3, 5) | 1.000 | 1.000 | 0.954 | 0.979 |
| (3, 2) | 0.995 | 0.979 | 0.908 | 1.000 | (3, 6) | 1.000 | 0.979 | 0.903 | 1.000 |
| (3, 3) | 1.000 | 1.000 | 0.964 | 0.995 | (3, 7) | 1.000 | 1.000 | 0.954 | 0.995 |
| (3, 4) | 0.995 | 1.000 | 0.774 | 1.000 | (3, 8) | 0.995 | 1.000 | 0.821 | 1.000 |
| (4, 1) | 0.990 | 1.000 | 0.928 | 0.969 | (4, 5) | 0.985 | 1.000 | 0.928 | 0.964 |
| (4, 2) | 0.953 | 0.953 | 0.845 | 0.915 | (4, 6) | 0.953 | 0.953 | 0.845 | 0.915 |
| (4, 3) | 0.995 | 0.974 | 0.821 | 1.000 | (4, 7) | 0.995 | 0.974 | 0.800 | 1.000 |
| (4, 4) | 0.954 | 0.985 | 0.872 | 0.933 | (4, 8) | 0.959 | 0.974 | 0.903 | 0.944 |
| (5, 1) | 1.000 | 1.000 | 0.918 | 1.000 | (5, 5) | 1.000 | 1.000 | 0.877 | 1.000 |
| (5, 2) | 1.000 | 1.000 | 0.882 | 1.000 | (5, 6) | 0.959 | 0.990 | 0.882 | 1.000 |
| (5, 3) | 1.000 | 1.000 | 0.928 | 1.000 | (5, 7) | 0.959 | 0.969 | 0.918 | 1.000 |
| (5, 4) | 1.000 | 1.000 | 0.944 | 1.000 | (5, 8) | 0.969 | 0.938 | 0.877 | 1.000 |
| (6, 1) | 1.000 | 1.000 | 0.938 | 1.000 | (6, 5) | 0.979 | 1.000 | 0.831 | 1.000 |
| (6, 2) | 1.000 | 1.000 | 0.856 | 1.000 | (6, 6) | 0.974 | 0.985 | 0.872 | 1.000 |
| (6, 3) | 1.000 | 1.000 | 0.836 | 1.000 | (6, 7) | 0.985 | 0.974 | 0.944 | 1.000 |
| (6, 4) | 1.000 | 0.990 | 0.887 | 1.000 | (6, 8) | 0.969 | 0.892 | 0.713 | 1.000 |
| (7, 1) | 1.000 | 1.000 | 0.913 | 0.985 | (7, 5) | 0.995 | 1.000 | 0.795 | 0.985 |
| (7, 2) | 0.995 | 0.985 | 0.882 | 1.000 | (7, 6) | 0.995 | 0.949 | 0.882 | 1.000 |
| (7, 3) | 1.000 | 1.000 | 0.944 | 0.990 | (7, 7) | 0.974 | 0.969 | 0.923 | 0.985 |
| (7, 4) | 0.995 | 1.000 | 0.836 | 1.000 | (7, 8) | 0.985 | 0.969 | 0.959 | 0.990 |
| (8, 1) | 0.985 | 1.000 | 0.918 | 0.959 | (8, 5) | 0.990 | 1.000 | 0.851 | 0.959 |
| (8, 2) | 0.953 | 0.953 | 0.876 | 0.922 | (8, 6) | 0.915 | 0.922 | 0.860 | 0.915 |
| (8, 3) | 0.995 | 0.954 | 0.764 | 1.000 | (8, 7) | 0.979 | 0.887 | 0.805 | 0.995 |
| (8, 4) | 0.959 | 0.985 | 0.867 | 0.944 | (8, 8) | 0.944 | 0.985 | 0.887 | 0.933 |

## 6.6 $F_2$-score

Table 9: $F_2$-scores of various PM methods and DGM for all 64 2D rotor simulations with various amounts of meandering, fibrosis and noise. Minimal values are marked in blue (PM) and red (DGM).

| rotor (row,column) | $F_2$(PM1) | $F_2$(PM2) | $F_2$(PM3) | $F_2$(DGM) | rotor (row,column) | $F_2$(PM1) | $F_2$(PM2) | $F_2$(PM3) | $F_2$(DGM) |
|---|---|---|---|---|---|---|---|---|---|
| (1, 1) | 0.951 | 1.000 | 0.929 | 1.000 | (1, 5) | 0.998 | 1.000 | 0.938 | 1.000 |
| (1, 2) | 1.000 | 1.000 | 0.882 | 1.000 | (1, 6) | 1.000 | 1.000 | 0.877 | 1.000 |
| (1, 3) | 1.000 | 1.000 | 0.947 | 1.000 | (1, 7) | 1.000 | 1.000 | 0.944 | 1.000 |
| (1, 4) | 1.000 | 1.000 | 0.904 | 1.000 | (1, 8) | 1.000 | 1.000 | 0.903 | 1.000 |
| (2, 1) | 0.939 | 1.000 | 0.936 | 1.000 | (2, 5) | 1.000 | 1.000 | 0.933 | 1.000 |
| (2, 2) | 1.000 | 1.000 | 0.890 | 1.000 | (2, 6) | 1.000 | 1.000 | 0.895 | 1.000 |
| (2, 3) | 1.000 | 1.000 | 0.954 | 1.000 | (2, 7) | 1.000 | 1.000 | 0.946 | 1.000 |
| (2, 4) | 1.000 | 0.985 | 0.875 | 1.000 | (2, 8) | 1.000 | 0.990 | 0.869 | 1.000 |
| (3, 1) | 1.000 | 0.992 | 0.963 | 0.979 | (3, 5) | 1.000 | 0.991 | 0.963 | 0.979 |
| (3, 2) | 0.994 | 0.979 | 0.918 | 1.000 | (3, 6) | 1.000 | 0.978 | 0.913 | 1.000 |
| (3, 3) | 1.000 | 0.999 | 0.943 | 0.995 | (3, 7) | 1.000 | 1.000 | 0.937 | 0.995 |
| (3, 4) | 0.995 | 1.000 | 0.699 | 1.000 | (3, 8) | 0.995 | 1.000 | 0.731 | 1.000 |
| (4, 1) | 0.981 | 0.987 | 0.941 | 0.969 | (4, 5) | 0.985 | 0.988 | 0.942 | 0.964 |
| (4, 2) | 0.962 | 0.951 | 0.864 | 0.931 | (4, 6) | 0.962 | 0.951 | 0.864 | 0.931 |
| (4, 3) | 0.995 | 0.960 | 0.768 | 1.000 | (4, 7) | 0.995 | 0.952 | 0.755 | 1.000 |
| (4, 4) | 0.918 | 0.882 | 0.761 | 0.936 | (4, 8) | 0.921 | 0.872 | 0.782 | 0.945 |
| (5, 1) | 0.986 | 0.994 | 0.931 | 1.000 | (5, 5) | 0.918 | 0.959 | 0.884 | 1.000 |
| (5, 2) | 1.000 | 1.000 | 0.903 | 1.000 | (5, 6) | 0.808 | 0.856 | 0.738 | 1.000 |
| (5, 3) | 1.000 | 0.994 | 0.908 | 1.000 | (5, 7) | 0.748 | 0.647 | 0.597 | 1.000 |
| (5, 4) | 1.000 | 0.965 | 0.870 | 1.000 | (5, 8) | 0.730 | 0.597 | 0.516 | 1.000 |
| (6, 1) | 1.000 | 0.998 | 0.947 | 1.000 | (6, 5) | 0.921 | 0.953 | 0.824 | 1.000 |
| (6, 2) | 1.000 | 1.000 | 0.878 | 1.000 | (6, 6) | 0.855 | 0.825 | 0.682 | 1.000 |
| (6, 3) | 1.000 | 0.997 | 0.853 | 1.000 | (6, 7) | 0.769 | 0.715 | 0.661 | 1.000 |
| (6, 4) | 1.000 | 0.955 | 0.818 | 1.000 | (6, 8) | 0.730 | 0.568 | 0.420 | 1.000 |
| (7, 1) | 1.000 | 0.990 | 0.928 | 0.985 | (7, 5) | 0.995 | 0.928 | 0.792 | 0.985 |
| (7, 2) | 0.995 | 0.980 | 0.894 | 1.000 | (7, 6) | 0.892 | 0.793 | 0.721 | 1.000 |
| (7, 3) | 0.997 | 0.984 | 0.915 | 0.990 | (7, 7) | 0.760 | 0.722 | 0.677 | 0.985 |
| (7, 4) | 0.994 | 0.970 | 0.738 | 1.000 | (7, 8) | 0.690 | 0.608 | 0.565 | 0.990 |
| (8, 1) | 0.985 | 0.987 | 0.930 | 0.959 | (8, 5) | 0.990 | 0.897 | 0.811 | 0.959 |
| (8, 2) | 0.962 | 0.949 | 0.890 | 0.937 | (8, 6) | 0.831 | 0.784 | 0.730 | 0.931 |
| (8, 3) | 0.995 | 0.905 | 0.706 | 1.000 | (8, 7) | 0.789 | 0.611 | 0.546 | 0.995 |
| (8, 4) | 0.923 | 0.830 | 0.743 | 0.945 | (8, 8) | 0.635 | 0.633 | 0.589 | 0.936 |